

A TOMOGRAPHICAL METHOD USING HOLOGRAPHIC INTERFEROMETRY FOR THE REGISTRATION OF THREE-DIMENSIONAL UNSTEADY TEMPERATURE PROFILES IN LAMINAR AND TURBULENT FLOW

W. Ostendorf<sup>1</sup>, F. Mayinger<sup>2</sup> and D. Mewes<sup>1</sup>

1. Institut für Verfahrenstechnik, Hannover, FRG  
2. Lehrstuhl A für Thermodynamik, München, FRG

Unsteady three-dimensional temperature profiles in laminar or turbulent flow are examined with the use of optical tomography. This method does not affect the fluid dynamics of the system. This optical method uses holographic interferometry to obtain exact readings of a three-dimensional temperature profile at any selected time. Transient heat transfer phenomenon can be observed in single-phase flow fields without any time delay. The method is applied to the mixing phenomenon that occurs while a heated liquid of small volume is injected into an agitated vessel of isothermal surrounding filled with the same liquid. Certain fluid elements with deviating temperatures are detected during the interval of macromixing. The method is also applied to more viscous fluids for the investigation of dissipation phenomenon occurring during laminar mixing in agitated vessels.

1. INTRODUCTION

Heat transfer causes temperature profiles that can be calculated by numerical methods for relatively simple boundary conditions in laminar flow. Measurement techniques are developed to obtain time-dependent indications of the temperature in turbulent flow at certain locations. The temperatures are indicated by sensors which more or less disturb the flow. The method of optical tomography was developed in order to examine unsteady three-dimensional temperature profiles in laminar or turbulent flow without any disturbance of the fluid element behaviour.

2. PRINCIPLE OF HOLOGRAPHIC INTERFEROMETRY

The principle of holographic interferometry has been discussed in detail by Mayinger and Panknin /1,2/. Therefore, only the fundamentals which are necessary for the use in tomography are described.

With the use of a beam splitter, a laser beam is divided into two parts. Then, both beams are expanded into parallel waves. Behind the test section, the object wave passing through the test section interferes with the reference wave on the

photographic plate (Fig.1a).

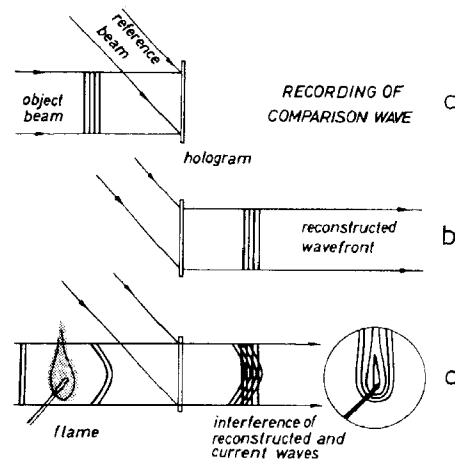


Fig.1 : Holographic interferometry (Real-Time-Method)

After processing, the plate, which is now called 'hologram', is illuminated by the reference wave only. The microscopic interference pattern of the hologram acts like a diffraction grating with variable grating constant. The transmitted light is a zero-order wave travelling in the direction of the reconstructed wave plus two first order waves. One of these first order waves travels in the same direction as the original object wave and has the same amplitude and the same phase distribution (Fig.1b).

When the temperature profile changes in the test section, due to the correlation between temperature and refractive index, the object wave experiences an additional phase shift. If the hologram is illuminated by the actual object wave and the reference wave, the both wave fronts interfere behind the hologram. The resulting interference pattern contains information about the temperature changes in the test section. It can be recorded by still or movie cameras (Fig.1c). This interference technique is called Real-Time-Method.

If the angle between the reference wave and the object wave is changed after processing the holographic plate, an even interference fringe pattern will be seen before the temperature is changed. Now the changes of the temperature profile in the test section are expressed in a deformation of pretended interference fringes, not in a formation of fringes. This special technique guarantees an easy treatment of the interference pictures and a better information density.

### 3. EVALUATION OF THE INTERFEROGRAM

The phase shift between the actual and the reconstructed object waves, which becomes visible by the deformation of the interference fringes, is caused by the change of the optical path length in the test volume. The correlation between the phase shift and the optical path length can be expressed by the following interferometer equation:

$$\phi = \int_L \Delta n(x, y, z, t) dy \quad (1)$$

In this integral equation, L is the integration path along a light beam in the test volume.

The phase shift is related only to the integral change of the optical path length along the light. Therefore, only an unique correlation between the phase shift and the refractive index is obtained, if the refractive index is constant along the light path. Only a 2-dimensional field can be determined from one interferogram. In spite of this restriction, a 3-dimensional field can be reconstructed, if the test volume is illuminated from different viewing angles as shown schematically in Fig.2.

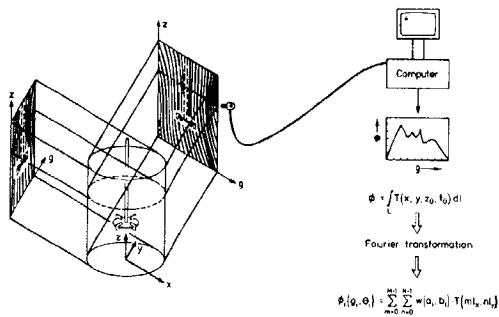


Fig.2 : Principle of tomography

Several integral values of the unknown refractive index function are obtained, if different projections of the unknown refractive index profile are measured in the test volume.

$$\phi_i(\rho, \theta, z, t) = \int_L \Delta n(x, y, z, t) dl \quad (2)$$

By transforming Eq.2 into a set of summation equations, the refractive index values can be

calculated. This transformation is based on the "Whittaker-Shannon-Sampling Theorem". More details about this evaluation technique are mentioned by Lübke /3/, Mewes, Ostendorf /4/ and Mayinger, Lübke /5/.

In order to obtain a reconstruction of high quality, a lot of different projections are necessary. The number of different projections, however, is limited. The heat transfer in the test volume is unsteady and therefore the volume has to be illuminated from all different viewing angles simultaneously. The indicated phase shifts are related to different viewing angles and the same time. The optical setup and the limited intensity of laser light density allows an illumination of the test volume from a few viewing angles only.

For the used tomographic evaluation technique, four viewing angles are necessary to obtain a reconstruction of sufficient quality.

In Fig.2, the practical evaluation is shown as well. The intersection points between the interference fringes and discrete levels are digitized and recorded. Consequently, the 3-dimensional field in the test volume is reduced to several 2-dimensional fields. The distance between two adjacent levels can be reduced to very small values. Thus, the vertical expansion of the field can be reconstructed as well. The coordinates of the intersection points of all interference fringes are used to calculate the phase shift along the radius of the test volume. The phase shifts of all irradiation angles are the input data for the tomography evaluation technique. Finally, the determined refractive index field is transformed into a temperature field for each cross section of the vessel. In Fig.3 such a temperature field is shown for a discrete level in the test volume.

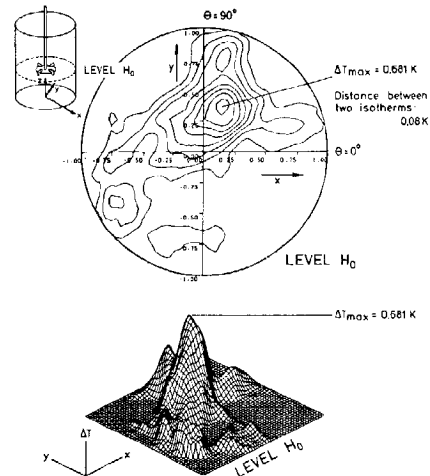


Fig.3 : Reconstructed temperature field

### 4. EXPERIMENTAL SETUP

The experimental setup shown in Fig.4 is designed to measure the temperature fields in mixing vessels.

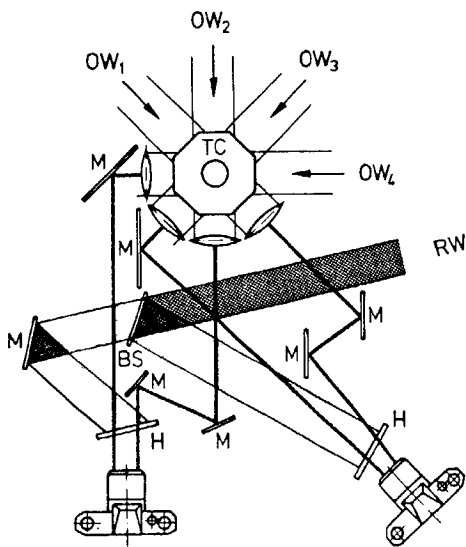


Fig.4 : Optical setup

The test chamber (TC) consists of an octagonal glass chamber and a glass cylinder. This cylinder is located in the center of the glass chamber and it is sealed from the exterior. The mixing process takes place in the glass cylinder. The entire test chamber is filled with liquids with a refractive index equal to the index of the used glass. This property of the liquids is necessary, because the light beams passing through the test chamber are not allowed to refract. Glycerin of 99.5% concentration or a solution of palatinol and benzene are used as liquids. Palatinol is a mixture of different phthalic esters. The test chamber is illuminated by four light beams of parallel expansion, which are scattered about  $45^\circ$  ( $OW_1-OW_4$ ). These object waves are focussed when leaving the test chamber. In order to expose the holographic plate and to take a picture of the interference pattern at a short exposure rate, a high light intensity is necessary. Two object waves that interfere with one reference wave (RW) interfere upon the holographic plates (H). The light source for all partial waves is an Argon-Ionen-Laser ( $P = 3.0 \text{ W}$ ,  $\lambda_0 = 514\text{nm}$ ).

## 5. EXPERIMENTAL CONDITIONS

The described tomographic evaluation technique has been applied successfully to measure the changes of temperature profiles in agitated vessels. A closed, cylindrical, unbafeled mixing vessel with a flat bottom is used for the experiments. The diameter of the vessel is 95mm. The variation of the number of revolutions of the 4-blade rushton turbine resulted in Reynolds-numbers  $100 < Re < 1000$ . In order to create an unsteady temperature profile in the agitated vessel, a heated liquid volume of about 3ml is injected. The added liquid and the liquid in the vessel consist of the same solution of palatinol

and benzene. The initial temperature difference between the liquids is about  $\Delta T = 0.85^\circ\text{C}$ .

## 6. DETERMINATION AND OBSERVATION OF MACROSCOPIC FLUID ELEMENTS IN AN AGITATED VESSEL

The mixing process in the agitated vessel is caused by diffusion and convective transport processes between fluid elements of different sizes and different concentration or temperature. The fluid elements to be mixed are divided into smaller fluid elements by the momentum transfer in the surroundings of the stirrer. These macroscopic fluid elements are separated gradually into decreasing elements such as eddies. During this process called macromixing the interfacial area between the components is expanded. When the fluid elements reach a certain size (microscopic elements), the inhomogeneity existing between the fluid elements is reduced by molecular transport processes.

### 6.1. Formation Of Fluid Elements In The Agitated Vessel

As an example, the formation of fluid elements is shown with the results of one series of experiments. The Reynolds-number is  $Re = 600$ . As first, the added liquid remains close to the surface of the vessel liquid, because its density is smaller than the density of the vessel liquid. Due to the secondary fluid flow caused by the movement of the stirrer, the added liquid moves along the stirrer shaft to the stirrer, as it is shown in Fig.5.

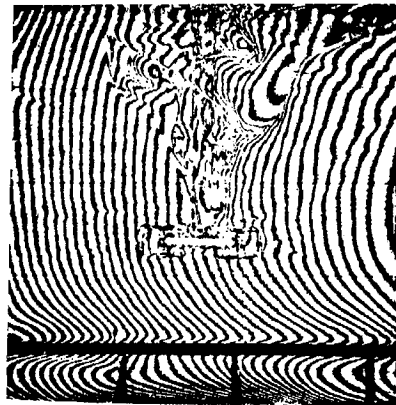


Fig.5 : Interferogramm of the mixing process in an agitated vessel. 6.5s after adding a heated volume of liquid

Outside of a conical volume near the shaft of the stirrer, the pattern of the interference fringes is undisturbed. For the examined time, the observed interference pattern indicates that no heated liquid has reached the area far away from the stirrer. It remains in the conical volume near the stirrer shaft.

The heated liquid is moving downward, as indicated by the temperature profiles in Fig.6. The time-dependent changes of the temperatures at the stirrer level are shown.

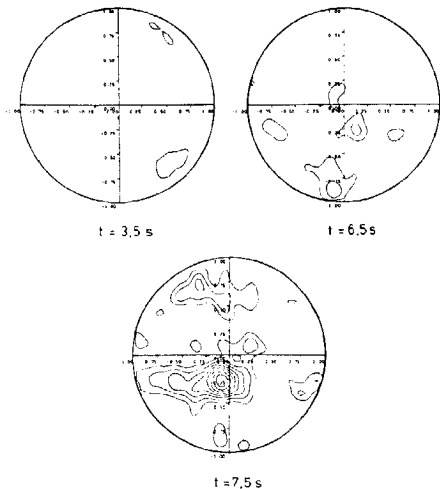


Fig.6 : Time-dependent change of the temperature at the stirrer level.  $\Delta T = 0.02 \text{ }^\circ\text{C}$

After durations of  $t = 3.5\text{ s}$  and  $t = 6.5\text{ s}$  the temperature profile of the examined cross section is nearly independent of the location. After the duration of  $t = 7.5\text{ s}$ , an area of relatively high temperature has been formed. This area can be interpreted as a plane cut through a liquid volume of relatively high temperature. The limit between the liquid volume and its environment is defined by the turning points of the temperature profiles along discrete sections to the ring shaped isotherms. In Fig.7 the determination of the limit between the heated liquid volume and its environment is schematically shown.

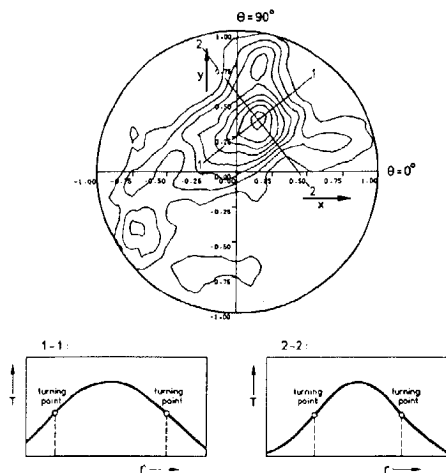


Fig.7 : Determination of a limit between a heated liquid volume and its environment

In order to obtain the spatial expansion of the liquid volume, the temperature profiles at several levels are reconstructed in the immediate vicinity of the stirrer.

The plane cuts through this liquid volume at six superimposed levels are marked in Fig.8 in order to present a picture of the vertical expansion of the liquid volume. The temperature difference between adjacent isotherms amounts to  $\Delta T = 0.02 \text{ }^\circ\text{C}$ .

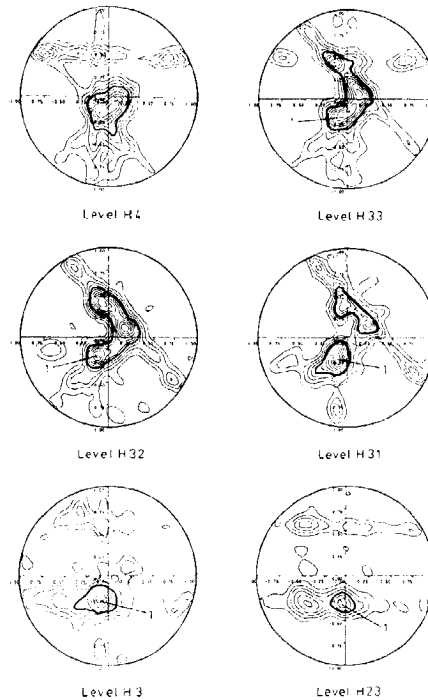


Fig.8 : Reconstructed temperature profiles after a duration of  $t = 7.5\text{ s}$  after adding the heated liquid volume.

In the cross section of the stirrer (H31), the volume flow of the liquid is divided into two smaller streams of liquid of different vertical expansions. The vertical position of the other mentioned temperature profiles in the agitated vessels are presented in Fig.9.

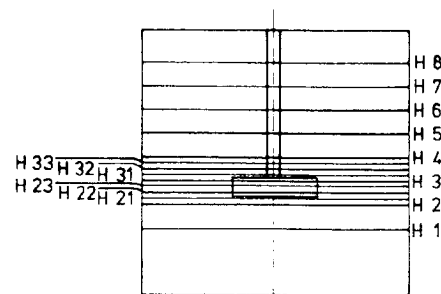


Fig.9 : Position of the different levels in the agitated vessel

In order to give an impression of the spatial shape of the described liquid volume, a picture of the volume is given in Fig.10.

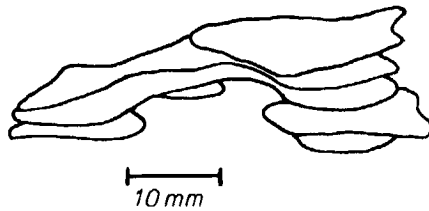


Fig.10 : Picture of a reconstructed liquid volume

While the described liquid volume passes through the rotating stirrer blades, single macroscopic fluid elements are torn away from it. These correspond to the eddies during the so-called "macromixing", which are formed by the phenomenon of segregation.

### 6.2. Change Of The Fluid Element Shape During Mixing

Two fluid elements are formed from the liquid volume 1 marked in Fig.9 during the first 8s of mixing time. Their plane expansions at the different levels of the agitated vessel are marked in Fig.11. They are identified with the numbers 1a and 1b.

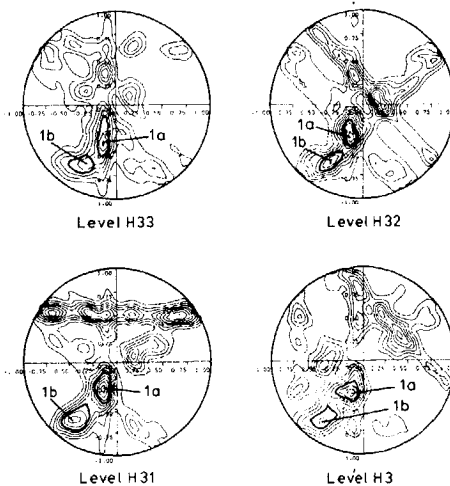


Fig.11 : Reconstructed temperature profiles after a duration of  $t = 8.0 \text{ s}$ ,  $\Delta T = 0.02 \text{ }^\circ\text{C}$

The fluid element 1a is nearly 10mm high and its shape is elongated. The fluid element 1b is about 9mm high and its volume amounts to nearly  $3\text{cm}^3$ . Its shape is elongated as well. The pictures of these two fluid elements are shown in Fig.12.

After their formation ( $\Delta t = 0.5\text{s}$ ), the two fluid elements are still separated at the levels H4 and H33. However, at the levels H32 and H31 they are already united (Fig.13).

This fast coalescence of the fluid elements is caused by their boundary area, which has no phase-separating character. The liquid inside and outside of the fluid element has the same composition. Only the temperature is different. Therefore, there is no phase boundary in the sense

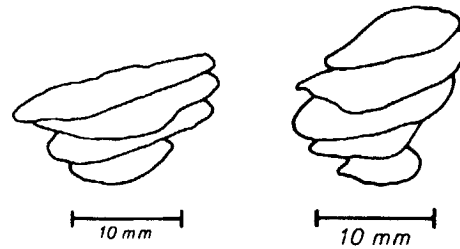


Fig.12 : Reconstructed fluid elements 1a and 1b

of fluid dynamics. There is no resistance against separation and coalescence. Adjacent fluid elements leaving the turbulent range in the immediate vicinity of the stirrer are soon united.

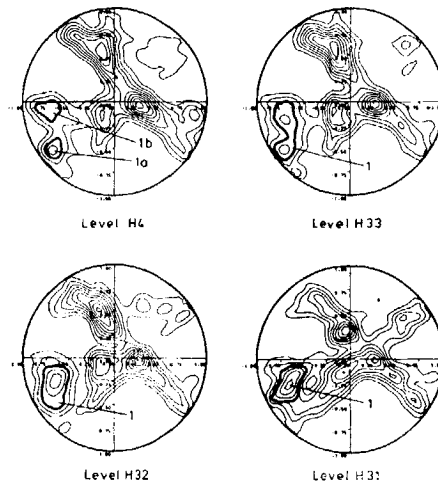


Fig.13 : Reconstructed temperature profiles after a duration of  $t = 8.5\text{s}$ ,  $\Delta T = 0.02 \text{ }^\circ\text{C}$

### 7. INVESTIGATION OF DISSIPATION PHENOMENON OCCURRING IN LAMINAR MIXING

The heat transfer in a mixing vessel is an instationary process. Because of the complexity of the spatial velocity field, so far only theoretical-numerical methods are available to investigate the heat transport. Brauer and Thiele /6/ as well as Brauer /7/ used a simple model of a cylindrical stirrer to investigate the influence of energy dissipation in laminar mixing on the structure of the temperature fields. Due to their simplified assumption, Brauer and Thiele obtained axial and symmetrical velocity and temperature fields. One of their calculated temperature fields is presented in Fig.14. The Prandtl-number is about  $Pr=100$  and the Reynolds-number amounts to  $Re=5.1$ .

After a certain mixing time (Fourier-number  $Fo = 0.0054$ ) the liquid increases its temperature due to dissipative effects in the immediate vicinity of the stirrer. The heat flux near the vessel wall is caused by the different

temperatures of the liquid and the vessel wall at the beginning of the mixing.

In order to apply optical tomography for a measurement of the temperature fields produced by dissipation, a high quantity of mechanical energy has to be transferred from the stirrer to the liquid. Therefore, a highly viscous liquid of 99.5% glycerine and 0.5% water ( $Pr=10000$ ) is used in the experiments.

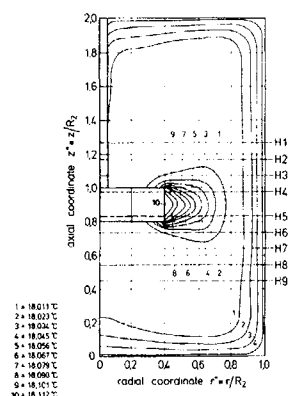


Fig.14 : Temperature field in a mixing vessel

During the mixing time of  $t=140$  s ( $Fr = 0.0054$ ), the liquid is heated as shown in Fig.15 for certain cross sections. The geometrical proportion of the vessel and the stirrer are similar to those shown in Fig.14. The Reynolds-number of the evaluated test series is  $Re=5.1$ .

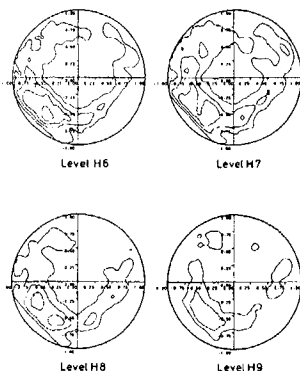


Fig.15 : Reconstructed temperature fields caused by dissipation.  $\Delta T = 0.01$  °C

At the cross-sections located at levels H6 to H9 (see Fig.14) the liquid was heated in a ring shaped area.

In radial direction, this area nearly extends from the edge of the stirrer to the vessel wall. Far away from the stirrer, at the levels H8 and H9, the radial expansion of the ring shaped area has been decreased. Consequently the temperature differences decrease as well.

A comparison between these results and the ones obtained by Brauer and Thiele shows that the axial and radial expansion of the heated area is much larger than the calculated one in Fig.14 and that the reconstructed rise in temperature is

higher than the one indicated by Brauer and Thiele.

The reason for these discrepancies is the fact that the liquid assumed by Brauer and Thiele is not as viscous as the liquid used in our experiments. Therefore, the velocity of the stirrer necessary to adjust a Reynolds-number of  $Re=5.1$  is different. Consequently the secondary flux, which is responsible for the heat transfer, is more extensive than the one assumed by Brauer and Thiele in their investigation.

In addition to the improvement of the heat transfer, the specific transferred mechanical energy is increased by the higher velocity of the stirrer. Therefore, the measured rise in temperature is higher than the one calculated by Brauer and Thiele. Comparing the measured mechanical energy added to the liquid by the stirrer movement and the heating of the liquid, the coincidence is satisfactory.

#### NOMENCLATURE

$n$	refractive index	-
$n_o$	speed of rotation	1/min
$r_o$	radius	m
$R_2$	radius of the vessel	m
$R_1$	radius of the stirrer	m
$t$	time	s
$T$	temperature	°C
$\Phi$	phase shift	m
$\lambda_o$	wave length	m
$\rho, \theta, z$	cylindrical coordinates	

#### Dimensionless Parameters

$$Re = \frac{n_o (2R_1)^2}{\nu} \quad \text{Reynolds-number}$$

#### REFERENCES

- Panknin, W.: Einige Techniken und Anwendungen der holographischen Durchlichtographie, Chemie Technik 3 (1974), 219/225
- Mayinger, F., Panknin, W.: Holography in heat and mass transfer, Proc. 5th Int. Heat Transf. Conf., Tokio, VI, 1974
- Lübbe, D.: Ein Messverfahren für instationäre, dreidimensionale Verteilungen und seine Anwendung auf Mischvorgänge, D. thesis, University Hannover, 1982
- Mewes, D., Ostendorf, W.: Einsatz tomographischer Messverfahren in der Verfahrenstechnik, Chem. Ing. Techn. 55 (1983) 11, 856/864
- Mayinger, F., Lübbe, D.: Ein tomographisches Messverfahren und seine Anwendung auf Mischvorgänge und Stoffaustausch, Wärme- und Stoffübertragung 18(1984), 49/59
- Brauer, H., Thiele, H.: Leistungsbedarf und Wärmeübertragung beim Rühren im laminaren Strömungsbereich, Vt 5 (1971) 10, 420/428
- Brauer, H.: Wärmetransport in Rührgefäßen, Wärme- und Stoffübertragung 13 (1980), 105/113